

# *Lith6*: a new QTL for cholesterol gallstones from an intercross of CAST/Ei and DBA/2J inbred mouse strains<sup>1,2,5</sup>

Malcolm A. Lyons,<sup>3,\*</sup> Henning Wittenburg,<sup>4,\*</sup> Renhua Li,<sup>\*</sup> Kenneth A. Walsh,<sup>\*</sup> Monika R. Leonard,<sup>†</sup> Ron Korstanje,<sup>\*</sup> Gary A. Churchill,<sup>\*</sup> Martin C. Carey,<sup>†</sup> and Beverly Paigen<sup>5,\*</sup>

The Jackson Laboratory,<sup>\*</sup> Bar Harbor, ME 04609; and Department of Medicine,<sup>†</sup> Harvard Medical School, Division of Gastroenterology, Brigham and Women's Hospital, Harvard Digestive Diseases Center, Boston, MA 02115

**Abstract** A complex genetic basis determines the individual predisposition to develop cholesterol gallstones in response to environmental factors. We employed quantitative trait locus/loci (QTL) analyses of an intercross between inbred strains CAST/Ei (susceptible) and DBA/2J (resistant) to determine the subset of gallstone susceptibility (*Lith*) genes these strains possess. Parental and first filial generation mice of both genders and male intercross offspring were evaluated for gallstone formation after feeding a lithogenic diet. Linkage analysis was performed using a form of multiple interval mapping. One significant QTL colocalized with *Lith1* [chromosome (chr) 2, 50 cM], a locus identified previously. Significantly, new QTL were detected and named *Lith10* (chr 6, 4 cM), *Lith6* (chr 6, 54 cM), and *Lith11* (chr 8, 58 cM). Statistical and genetic analyses suggest that *Lith6* comprises two QTL in close proximity. Our molecular and genetic data support the candidacy of peroxisome proliferator-activated receptor  $\gamma$  (*Pparg*) and *Slc21a1*, encoding *Pparg*, and the basolateral bile acid transporter SLC21A1 (*Slc21a1/Oatp1*), respectively, as genes underlying *Lith6*.—Lyons, M. A., H. Wittenburg, R. Li, K. A. Walsh, M. R. Leonard, R. Korstanje, G. A. Churchill, M. C. Carey, and B. Paigen. *Lith6*: a new QTL for cholesterol gallstones from an intercross of CAST/Ei and DBA/2J inbred mouse strains. *J. Lipid Res.* 2003. 44: 1763–1771.

**Supplementary key words** quantitative trait locus • *Castaneus* • *Lith* genes • cholelithiasis • *Pparg* • *Slc21a1* mice

Studies of model (1–3), animal (4–6), and human biles (7–9) have greatly contributed to the elucidation of the pathophysiology of cholesterol gallstone formation (cholelithiasis). Investigation of both human (10) and mouse models (11) demonstrated that a complex genetic basis determines the individual predisposition to develop cholesterol gallstones in response to environmental factors (12). Advancement of our understanding of cholesterol homeostasis and of the mechanisms of bile formation enables us to identify the primary genetic determinants of

cholesterol gallstone formation (13) and may lead to improved management and ultimately prevention of this prevalent and costly disorder (14). To this end, we employed quantitative trait locus/loci (QTL) analysis to define genomic regions associated with cholelithiasis in inbred mice. Our ultimate goal is to identify genes that carry polymorphisms determining cholesterol gallstone susceptibility (i.e., *Lith* genes) (13, 15). Including this report, 11 major QTL for cholelithiasis, named *Lith1* through *Lith11* (11, 16–20), have been reported. Each gallstone-susceptible inbred mouse strain carries only a subset (21) of all gallstone susceptibility alleles. Therefore, to confirm loci from previous studies and to identify the entire ensemble of *Lith* loci in inbred mice, we are conducting a further series of QTL crosses between cholesterol gallstone-susceptible and -resistant inbred mouse strains that were selected on the basis of a large strain survey (22).

Abbreviations: *Abcb11*, bile salt export pump (*Bsep*); *Apobec1*, apolipoprotein B mRNA editing complex 1; CAST, CAST/Ei; *Cav*, caveolin; *Cav2*, caveolin 2; *Cfr*, cystic fibrosis transmembrane conductance regulator; ChMC, cholesterol monohydrate crystal; chr, chromosome; CI, confidence interval; CSI, cholesterol saturation index; *Cyp7a1*/CYP7A1, cholesterol 7 $\alpha$ -hydroxylase; D2, DBA/2J; F<sub>1</sub>, first filial generation; F<sub>2</sub>, second filial generation or intercross; *Lith*, lithogenic locus; LOD, logarithm of the odds ratio; *Lrp2*/LRP2, low density lipoprotein receptor-related protein 2; *Nr1h3*/NR1H3, nuclear oxysterol receptor, (*Lxra*/LXR $\alpha$ ); *Pparg*/PPAR $\gamma$ , peroxisome proliferator-activated receptor  $\gamma$ ; QTL, quantitative trait locus/loci; *Rxra*, retinoid X receptor  $\alpha$ ; *Slc21a1*/SLC21A1, solute carrier family 21A, common name *Oatp*/OATP, organic anion transporting polypeptide.

<sup>1</sup> Presented in part at the Digestive Diseases Week 2002, San Francisco, CA, and published as an abstract in *Gastroenterology* 2002; **122**: A626.

<sup>2</sup> DNA sequences cited in this manuscript have been submitted to GenBank with the following accession numbers: AY236532, AY236533, AY236534, AY236535, AY236530, AY236531, AY236528, AY236529, AY195869, AY195868, AY236536, and AY236537.

<sup>3</sup> Present address of M. A. Lyons: School of Biotechnology and Biomolecular Sciences, Biological Sciences Building, D26, Room 257, University of New South Wales, Sydney, 2052 Australia.

<sup>4</sup> Present address of H. Wittenburg: Department of Medicine II, University of Leipzig, Leipzig, Germany.

<sup>5</sup> To whom correspondence should be addressed.

e-mail: [bjp@jax.org](mailto:bjp@jax.org)

<sup>5</sup> The online version of this article (available at <http://www.jlr.org>) contains three supplemental tables.

Manuscript received 9 April 2003 and in revised form 29 May 2003.

Published, JLR Papers in Press, June 16, 2003.  
DOI 10.1194/jlr.M300149.JLR200

This intercross between the gallstone-susceptible inbred strain CAST/Ei (CAST) and the gallstone-resistant inbred strain DBA/2J (D2) confirmed the previously identified locus *Lith1* and detected three new *Lith* loci named *Lith6* [reported in abstract form (19)], *Lith10*, and *Lith11*. We provide evidence that *Lith6* represents a complex locus that is likely determined by two closely linked QTL, for which the candidate genes are *Pparg* and *Slc21a1*.

## MATERIALS AND METHODS

### Animals and diet

Animals, breeding protocols, and facilities have been described in detail elsewhere (23). At 6 to 8 weeks of age, mice were transferred from chow to the cholesterol gallstone-promoting [lithogenic (11, 22)] diet. Parental strains and first filial generation (F<sub>1</sub>) mice were fed the diet for 8 weeks, whereas second filial generation (F<sub>2</sub>) progeny consumed the diet for 10 weeks. Animals were allowed free access to food and water. All animals fasted 4 h prior to sacrifice by cervical dislocation. The Institutional Animal Care and Use Committees of The Jackson Laboratory and Harvard University approved all protocols.

### Phenotyping of hepatic and gallbladder biles

To define the physical-chemical sequences of cholesterol gallstones, we collected both gallbladder and hepatic biles from each strain. The gallbladders of the two strains were very small (D2, 4.5 ± 0.5 mg, ~4.5 μl; CAST, 6.5 ± 0.3 mg, ~6.5 μl). Parental male mice were fed the lithogenic diet for 4 weeks. Gallbladders were removed, punctured at the fundus, and bile collected. A second group of animals were anesthetized with intraperitoneal injections of a cocktail comprising xylazine (20 mg kg<sup>-1</sup>; Phoenix Pharmaceutical, Inc., St. Joseph, MO) and ketamine (100 mg kg<sup>-1</sup>; Fort Dodge Animal Health, Fort Dodge, IA) prior to the introduction of a biliary fistula introduced via the gallbladder fundus (24). Anesthesia was maintained with ketamine alone. Gallbladder bile was allowed to drain (5 min) prior to hepatic bile collection by gravity (60 min, 37 ± 0.5°C). Hepatic bile volume was determined gravimetrically (assuming a density of 1 g ml<sup>-1</sup>). Both gallbladder and hepatic biles were stored at -20°C and lipid analyses conducted as described (24).

### Cholesterol gallstones

To determine prevalence rates, mice of the parental strains CAST and D2 (n = 10 per gender and strain) and the reciprocal F<sub>1</sub> progeny (n = 10 per lineage male; n = 5 per lineage female) and male F<sub>2</sub> mice (n = 278) were phenotyped for cholesterol gallstones using standard methods (principally polarizing light microscopy) (5, 25). Opaque solid cholesterol gallstones were counted, air dried overnight, and weighed (5). In addition to the gallstone score (18, 24) assigned to bile samples, aggregated cholesterol monohydrate crystals (ChMCs) were semiquantified using a 0–4 scale, where 0 represented absence of aggregated crystals and 4 represented a gallbladder full of aggregated crystals. Livers were removed, frozen in liquid nitrogen, and stored at -80°C for isolation of mRNA.

### Genotyping and QTL analyses

Genotyping and parameters for QTL analyses have been previously described for this intercross (23). QTL analyses were performed using the multistage analysis of Sen and Churchill (26), whose application was described recently in detail (24). To determine the likelihood that a QTL comprised more than one locus linked to the respective phenotype, the QTL on chromosome

(chr) 2 and chr 6 were fit with models comprising one, two, or three QTL and a maximum logarithm of the odds ratio (LOD) score calculated for each. Employing permutation testing, we determined that increases of 2.0, 1.6, and 1.4 in the LOD score (ΔLOD) are the thresholds that define multiple QTL at the 95%, 90%, and 80% confidence levels, respectively.

### Candidate gene mapping and sequencing

From the mouse genome database (ENSEMBL), two candidate genes encoding Na<sup>+</sup>-independent solute (organic anion) carriers were identified on distal chr 6. *Slc21a1* was mapped to chr X using fluorescent in situ hybridization (27), whereas *Slc21a5* was mapped to its cytogenetic band on chr 6. Therefore, the T31 Mouse Radiation Hybrid Panel (Research Genetics, Huntsville, AL) was employed to map the positions of *Slc21a1* (*Oatp1*) and *Slc21a5* (*Oatp2*) following the recommendations of The Jackson Laboratory T31 Mouse Radiation Hybrid Database (<http://www.jax.org/resources/documents/cmdata/rhmap/rh.html>). As described (23), primer pairs that discriminated between the mouse and hamster genes were identified (*Slc21a1*, 5'-agt tat gag cta gtc aga gaa gag c-3' (forward) and 5'-gag gtg atg tct acc cta ttg c-3' (reverse); *Slc21a5*, 5'-ttc agt ccc ttc ttt cat tac tcc-3' (forward) and 5'-gga cta gtt ttc tcc cat tct tga-3' (reverse)). We sequenced cDNA and ~750 to 1,000 nucleotides proximal to the transcription start site of *Pparg* and *Slc21a1*, two key candidate genes for *Lith6*, using previously described methods (23).

### mRNA expression analyses

We evaluated hepatic mRNA expression profiles of candidate genes using quantitative (real-time) PCR. Expression differences between the parental strains (n = 5 per strain) could be regulated by elements lying within the QTL or by elements located elsewhere in the genome. To determine which was true, we selected F<sub>2</sub> progeny (n = 10–15 per genotype), which possessed identical alleles in the locus of interest but random combinations of alleles at all other loci. If differential expression between genotypes was confirmed in these F<sub>2</sub> groups, we concluded that regulatory elements must be located within the QTL region. As described elsewhere (23), primers were designed and verified and analyses performed. (Primer sequences are presented as supplementary data.)

### General statistical analyses

Data are presented as means ± SEM and were analyzed using Graphpad Prism (Windows v3.00, GraphPad Software, San Diego, CA). Continuous data (e.g., biliary secretion rates, mRNA expression) were analyzed using Student's *t*-test. Bonferroni post-test was applied to the analyses of mRNA expression data. *P* < 0.05 was considered significant.

## RESULTS

### Gallstone prevalence and distribution

Gallstone prevalence rates are presented in Fig. 1. Mice from the parental strains developed sandy (translucent) cholesterol gallstones, but no solid (opaque) gallstones (n = 40). In F<sub>1</sub> mice, females were gallstone resistant, but males were gallstone susceptible (0 vs. 100% prevalence); three F<sub>1</sub> males developed solid cholesterol gallstones. These results induced us to do the following with regard to the F<sub>2</sub> animals: 1) only males were phenotyped (the sexual dimorphism was not pursued); 2) the feeding regimen was prolonged to 10 weeks; 3) both sandy and solid stones

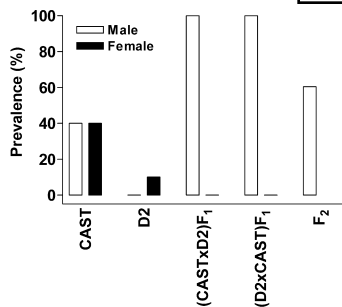


**Fig. 1.** Cholesterol gallstone prevalence rates among the parental strains, reciprocal first filial generations (F<sub>1</sub>s), and the second filial generation (F<sub>2</sub>). Procedures are described in Materials and Methods. The prevalence of the male F<sub>1</sub> groups was identical, indicating that gallstone susceptibility was not inherited through maternal or imprinted factors, and therefore, quantitative trait locus/loci (QTL) analyses could detect autosomal regions harboring *Lith* genes. Female F<sub>1</sub> animals were gallstone resistant; therefore, only male F<sub>2</sub> animals were used for QTL analyses.

were included to determine prevalence. Because no difference was observed between male reciprocal F<sub>1</sub> progeny, cholesterol gallstone susceptibility in this cross was not inherited by maternal or imprinted genetic factors.

The distributions of the gallstone phenotypes for the F<sub>2</sub> population are depicted in Fig. 2. Of those mice that developed solid gallstones (n = 58; Fig. 2A, B), the mean mass was 0.74 ± 0.67 mg (mean ± SD, range 0–3.2 mg) and the mean number was 5.4 ± 5.3 (mean ± SD, range 0–28). The gallstone score phenotype resembled a binary distribution (i.e., absence/presence) with approximately twice as many animals developing cholesterol gallstones (score = 2) as those not displaying phase separation (score = 0; Fig. 2C). Similar numbers of F<sub>2</sub> mice displayed no aggregated ChMCs (n = 117) or varying degrees of aggregated ChMCs (n = 154) (Fig. 2D).

### Biliary lipid analyses

**Hepatic bile.** Strains CAST and D2 displayed no differences in bile salt or phospholipid secretion rates over 60 min (Fig. 3A) or in total bile salt or phospholipid compositions (Fig. 3B), but CAST demonstrated significantly more cholesterol in hepatic bile compared with strain D2 ( $P < 0.01$ ; Fig. 3A, B). Male CAST mice displayed an increased rate of bile flow compared with D2 males ( $137.3 \pm 4.3$  vs.  $88.9 \pm 6.4 \mu\text{l min}^{-1} \text{kg}^{-1}$ , respectively; n = 7 per group,  $P < 0.0001$ ). Because CAST mice do not differ from D2 in total bile salt or phospholipid secretion rates, we inferred that the increased bile flow was most likely bile salt independent (28). Indeed, when we calculated the bile salt-independent bile flow by extrapolating bile salt output to a theoretical value of zero, CAST displayed greater flow than did D2 (Fig. 3C). This conclusion was supported further by the significantly lower total lipid concentration of hepatic bile displayed by strain CAST compared with strain D2 ( $1.85 \pm 0.14$  vs.  $2.41 \pm 0.16 \text{ g dl}^{-1}$ , respectively; n = 9–12 per group,  $P < 0.05$ ). The calculated cholesterol saturation indices (CSIs) of hepatic bile (3) showed that CAST exhibited a significantly greater CSI compared with D2 ( $P <$

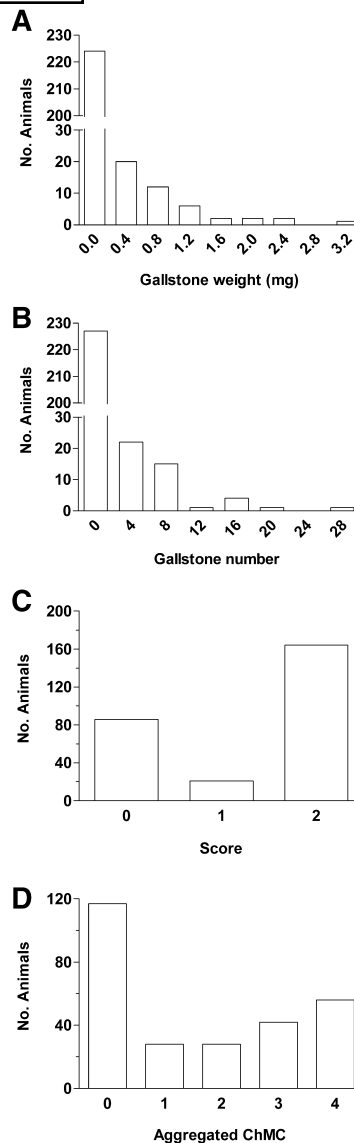


**Fig. 2.** Frequency distribution of gallstone phenotypes in the F<sub>2</sub> population after 10 weeks' consumption of the lithogenic diet. Only 58 F<sub>2</sub> mice developed solid gallstones; the majority of animals did not. A: Gallstone weight. B: Gallstone number. Therefore, a gallstone score (C) was assigned to the mice dependent upon absence (score = 0) or presence (score = 1) of cholesterol monohydrate crystals (ChMCs) (individual or aggregated) or presence of sandy and/or solid stones (score = 2). Hence, 164 mice possessed sandy and/or solid gallstones (C), the majority of which do not appear in A and B. Aggregated ChMCs (D) were semiquantified using a 0–4 scale (0 = absence, 4 = most severe presence). Ten mice developed sandy or solid stones but did not display individual or aggregated ChMCs at phenotyping.

0.0005; Fig. 3D), thus explaining its greater propensity to form cholesterol gallstones.

**Gallbladder bile.** Using individual D2 gallbladder biles (n = 3) and a pooled sample of CAST gallbladder bile, we confirmed that the CAST gallbladder bile CSI was greater than that of strain D2, in agreement with the hepatic bile CSI (Fig. 3D). Although the hepatic biles of both strains exhibited a CSI > 1, only the gallbladder bile of CAST mice ex-

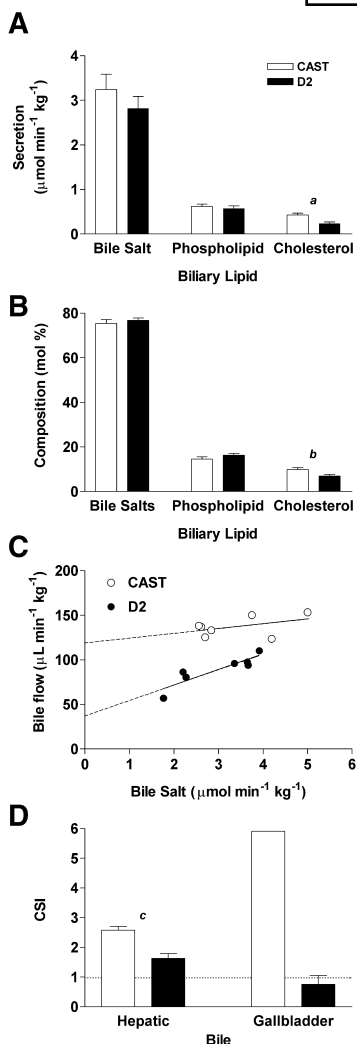


**Fig. 3.** Hepatic biliary lipid analyses of parental strains CAST (open) and D2 (filled) after 4 weeks' consumption of the lithogenic diet. An acute biliary fistula was fashioned and hepatic bile collected via the gallbladder for 60 min. Strain CAST displayed a significantly greater cholesterol secretion rate compared with strain D2 (A). The lipid composition of hepatic bile (B) indicated that CAST differed significantly from D2 only in cholesterol composition. CAST displayed higher bile salt-independent bile flow (C) compared with strain D2. The cholesterol saturation indices (CSIs, D) were calculated from the critical tables for taurocholate-rich bile (40). CAST displayed greater cholesterol saturation in hepatic bile compared with strain D2. This finding was confirmed for gallbladder bile (D) using individual D2 biles and a single sample of pooled bile from CAST mice. Note that the CSI < 1 for D2 gallbladder bile accounts for the gallstone resistance of this strain, whereas CSI >> 1 for strain CAST reflects its gallstone susceptibility. Despite all efforts to the contrary, the very high CSI of CAST gallbladder bile suggests the admixture of microscopic ChMCs in the sample. However, this does not affect the observation that CAST gallbladder bile was cholesterol supersaturated, whereas D2 gallbladder bile was not supersaturated. Data represent mean ± SEM; n = 8–12 per strain except D, gallbladder bile (n = 1, CAST; n = 3, D2). <sup>a</sup>P < 0.005; <sup>b</sup>P < 0.01; <sup>c</sup>P < 0.0005.

hibited a CSI > 1, thereby accounting for the gallstone susceptibility of this strain. It should be noted that the total lipid concentrations of hepatic biles were reversed in gallbladder biles (12.0 vs. 8.4 g dl<sup>-1</sup>, CAST vs. D2, respectively).

### QTL analyses

Three gallstone phenotypes (score, gallstone presence, stone weight) were used for genome-wide scans. Single QTL are presented in Fig. 4, but no gene interactions (epistasis) were detected. Suggestive (LOD > 2.2, P < 0.10) and significant (LOD > 3.3, P < 0.05) LOD scores were determined by permutation testing (29). Because the genome-wide scans for gallstone score and gallstone presence were similar, we present data for gallstone presence only. The gallstone presence scan (Fig. 4A) detected a significant QTL (*D2Mit94*, peak 52 cM) that confirmed the previously detected QTL, *Lith1* (11, 16), and a suggestive QTL on chr 6 (*D6Mit86*, peak 0 cM); the latter locus became significant

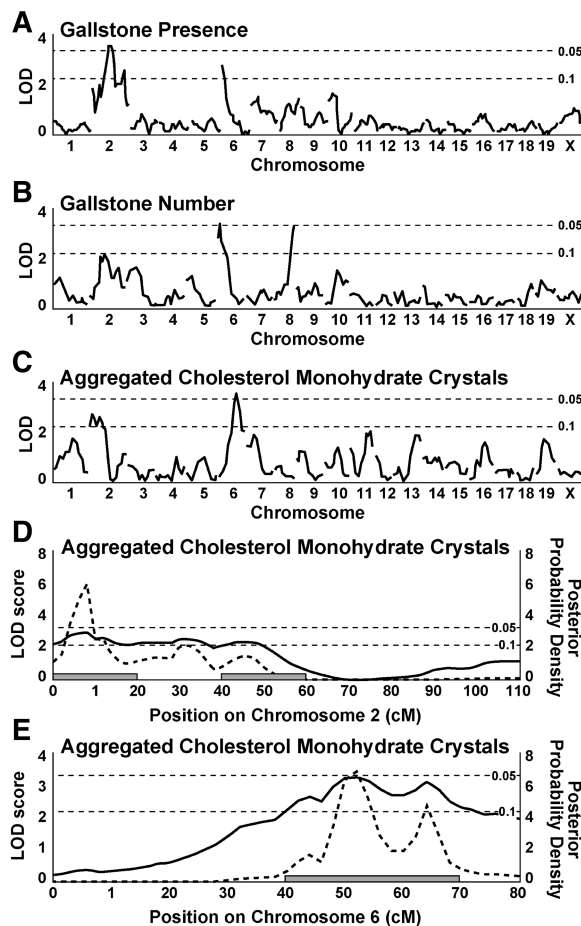


**Fig. 4.** Genome-wide QTL analyses for single cholesterol gallstone susceptibility loci in the F<sub>2</sub> population derived from strains CAST and D2. Chromosomes (chrs) 1 through X are represented numerically on the ordinate. The relative width of the space allotted for each chr reflects the number of simple sequence length polymorphism markers on each chr. The abscissa represents the logarithm of the odds ratio (LOD) score, the traditional metric of genetic linkage. The significant (LOD > 3.3, P < 0.05) and suggestive (LOD > 2.2, P < 0.10) levels of linkage were determined by permutation testing (29). Gallstone presence (0–1) is presented in A, gallstone number in B, aggregated ChMCs in C. Fine-mapping of the QTL for aggregated ChMCs on chr 2 (D) and chr 6 (E) are presented (solid line). The posterior probability density (broken curved line) is a likelihood statistic that gives rise to the 95% confidence intervals that are indicated by the gray bars (26). These data suggest that a third QTL exists on chr 2 and that at least two QTL exist on chr 6.

using gallstone number as the phenotype (peak 4 cM; Fig. 4B). The gallstone number analysis detected a significant QTL on distal chr 8 (*D8Mit88*, peak 58 cM). Finally, the genome-wide scan for aggregated ChMCs detected two suggestive QTL on chr 2 (proximal *D2Mit79*, peak 8 cM; distal *D2Mit94*, peak 46 cM) and one significant QTL on distal chr 6 (*D6Mit62*, peak 54 cM; Fig. 4C). However, the QTL fine-mapping of these loci suggests the presence of three QTL on chr 2 (Fig. 4D) and two to three QTL on chr 6 (Fig. 4E). Details of the QTL are presented in **Table 1**. We named the significant loci as follows: proximal chr 6, *Lith10*; distal chr 6, *Lith6*; and distal chr 8, *Lith11*.

Application of statistical models indicated that the QTL on chr 2 for gallstone presence was best fit by a two- or three-QTL model (95% and 90%, respectively; **Table 2**). The additional QTL likely reside at the proximal to mid region of chr 2 (Fig. 4D). Consistent with the QTL fine-mapping (Fig. 4E), the QTL on chr 6 for aggregated ChMCs suggested the existence of two closely linked QTL (80% confidence; Table 2), possibly accounting for the relatively large 95% confidence interval (CI) (40–70 cM) of *Lith6*.

At each simple sequence length polymorphism (SSLP) marker linked to a QTL, we determined the allele effect that shows which strain contributed the gallstone-susceptibility allele, the mode of inheritance, and the magnitude of the effect (**Fig. 5**). Gallstone susceptibility was determined by recessive D2 alleles at the QTL on proximal chr 2 (Fig. 5A), *Lith10* (Fig. 5C) and *Lith11* (Fig. 5E), by a dominant D2 allele at *Lith1* (Fig. 5B), and by a dominant CAST allele at *Lith6* (Fig. 5D).

### Candidate gene analyses

QTL analysis detects fundamental genetic differences in genes encoding key regulatory proteins (13). The mutations or polymorphisms may be in regulatory or coding re-

gions of the genome, or both, resulting in altered transcription levels, mRNA stability, or amino acid sequences. To initiate our search, we identified positional candidate genes within the 95% CIs of the QTL that possessed a direct or indirect role in lipid metabolism. We stipulate that our conclusions are based on mRNA expression data, but definitive exclusion of candidate genes requires cDNA sequencing.

### Candidate gene mapping

Both *Slc21a1* and *Slc21a5* mapped to chr 6, both with the highest anchor LOD to *D6Mit58* (67.0 cM). Therefore, we confirmed experimentally the localization of these genes on distal chr 6 in the *Slc21a* cluster.

### mRNA expression

Candidate genes were evaluated by determining whether their hepatic mRNA expression profiles (**Fig. 6**) were consistent with their known activities and allele effects. The QTL on distal chr 2 colocalized with *Lith1*, for which *Abcb11*, encoding the canalicular bile salt export pump (*Bsep*, 38.4 cM), is a strong candidate gene. *Abcb11* was located outside of the 95% CI of the QTL detected in this intercross, and, not surprisingly, we detected no difference in *Abcb11* mRNA (Fig. 6A) or in hepatic bile salt secretion rate (Fig. 3A). *Nr1h3* (*Lxra*, 40.4 cM), encoding the nuclear oxysterol receptor LXR $\alpha$ , lay within the 95% CI. After adjustment for multiple comparisons, the difference in *Nr1h3* expression between the parental strains was nonsignificant (Fig. 6A). Furthermore, genes whose transcription is activated by NRIH3, *Cyp7a1* and *Abcg5/Abcg8*, were not up-regulated in CAST (data not shown), as expected if *Nr1h3* determined *Lith1*. We concluded that both *Abcb11* and *Nr1h3* were not likely responsible for the QTL on distal chr 2 in this intercross. An association in humans was found recently between gallstones and a poly-

TABLE 1. QTL for cholesterol gallstone formation identified in the CAST  $\times$  D2 intercross

Locus (cM)	QTL Name	Phenotype	chr	LOD <sup>a</sup>	Peak (cM) (95% CI)	Variance (%)	Susceptible Allele, Inheritance <sup>b</sup>	Overlapping QTL (Ref. <sup>c</sup> )	Candidate Genes (cM)
<i>D2Mit79</i> (10.0)		Agg. ChMC	2	3.0	8 (0–20)	4.8	D2, Rec		<i>Cel<sup>d</sup></i> (16), <i>Rxra<sup>e</sup></i> (17)
<i>D2Mit94</i> (48.1)	<i>Lith1</i>	Agg. ChMC	2	2.4	46 (40–60)	3.9	D2, Dom	(16) <sup>f</sup>	<i>Nr1h3<sup>g</sup></i> (40.4), <i>Abcb11<sup>h</sup></i> (38.4)
<i>D2Mit94</i> (48.1)	<i>Lith1</i>	Stone presence	2	3.8	52 (40–60)	6.0	D2, Dom	(16) <sup>f</sup>	<i>Nr1h3</i> (40.4), <i>Abcb11</i> (38.4)
<i>D6Mit86</i> (0.5)	<i>Lith10</i>	Stone presence	6	2.8	0 (0–6)	4.6	D2, Rec		<i>Cav<sup>i</sup></i> (3.2), <i>Cav2<sup>j</sup></i> (3.2), <i>Cftr<sup>k</sup></i> (3.1)
<i>D6Mit86</i> (0.5)	<i>Lith10</i>	Stone number	6	3.6	4 (0–10)	5.8	D2, Rec		<i>Cav</i> (3.2), <i>Cav2</i> (3.2), <i>Cftr</i> (3.1)
<i>D6Mit62</i> (58.0)	<i>Lith6</i>	Agg. ChMC	6	3.8	54 (40–70)	5.2	CAST, Dom		<i>Pparg<sup>l</sup></i> (52.7), <i>Apobec1<sup>m</sup></i> (54.5), <i>Slc21a<sup>n</sup></i> (67)
<i>D8Mit88</i> (58.0)	<i>Lith11<sup>o</sup></i>	Stone number	8	3.3	58 (48–60)	5.2	D2, Rec		

chr, chromosome; CI, confidence interval; cM, centimorgan; LOD, logarithm of the odds ratio; QTL, quantitative trait locus.

<sup>a</sup> Using permutation analyses, suggestive QTL LOD  $\geq$  2.2, significant QTL LOD  $\geq$  3.3.

<sup>b</sup> Susceptible allele and mode of inheritance: Rec, recessive; Dom, dominant.

<sup>c</sup> Reference.

<sup>d</sup> Carboxyl ester lipase.

<sup>e</sup> Retinoid X receptor.

<sup>f</sup> Reference 16 and unpublished data, Wittenburg, Carey, and Paigen.

<sup>g</sup> Nuclear oxysterol receptor, common name *Lxra*.

<sup>h</sup> Canalicular bile salt export pump, common name *Bsep*.

<sup>i</sup> Caveolin.

<sup>j</sup> Caveolin 2.

<sup>k</sup> Cystic fibrosis transmembrane conductance regulator.

<sup>l</sup> Peroxisome proliferator activated receptor  $\gamma$ .

<sup>m</sup> Apolipoprotein B mRNA editing complex 1.

<sup>n</sup> Solute carrier family 21a gene cluster encoding members 1 (*Oatp1*), 5 (*Oatp2*), 7 (*Oatp3*), and 10 (*Oatp4*).

<sup>o</sup> QTL detected with second filial generation (F<sub>2</sub>) lineage as covariate.

TABLE 2. Determination of number of loci on chrs 2 and 6 using models describing one, two, and three QTL

Phenotype	chr	Model <sup>a</sup>					Number of QTL
		LOD <sub>1</sub>	LOD <sub>2</sub>	Δ LOD	LOD <sub>3</sub>	Δ LOD	
Stone presence	2	3.1	5.2	2.1	7.0	1.8	3
Agg. ChMC	6	3.7	5.1	1.4	5.6	—	2

ChMC, cholesterol monohydrate crystal. Using permutation analyses for an intercross of 278 mice, we determined that increases of 2.0, 1.6, and 1.4 or greater in the LOD score between models are the thresholds used to declare multiple QTL at the 95%, 90%, and 80% confidence levels, respectively. The data indicate that three QTL likely exist on chr 2 that determine the gallstone presence phenotype. Similarly, the data suggest the existence of two QTL for the aggregated ChMC phenotype.

<sup>a</sup> LOD<sub>1</sub> is the LOD score calculated for the one-QTL model; LOD<sub>2</sub> refers to the two-QTL model, and LOD<sub>3</sub> refers to the three-QTL model; ΔLOD is the difference between the respective models.

morphism in *LRP2* (30), whose homologous mouse gene, *Lrp2*, maps to this QTL, but hepatic expression is not substantial (31). Although we were able to amplify the transcript from liver tissue, we failed to detect any differential expression (23). Overall, we conclude that *Lrp2* is unlikely to be responsible for this QTL.

Of the remaining candidate genes, only *Pparg* and *Slc21a1*, both candidates for *Lith6*, displayed expression that was dictated by genotype in both the parental strains and F<sub>2</sub> progeny (Fig. 6B, C). Strain D2 exhibited ~5-fold greater expression of *Pparg* compared with strain CAST; F<sub>2</sub> progeny with D2 alleles at *Lith6* exhibited 13-fold higher expression compared with F<sub>2</sub> progeny with CAST alleles at that locus. Similarly, strain D2 displayed 2.5-fold higher expression of *Slc21a1* (*Oatp1*) compared with strain CAST; F<sub>2</sub> progeny with D2 alleles at *Lith6* exhibited 2.7-fold higher expression compared with F<sub>2</sub> progeny with CAST alleles. We postulate that altered expression of *Pparg* and *Slc21a1* might affect the concentration of intracellular bile salts and the availability of cholesterol for biliary secretion.

### Sequence analyses

No sequence differences causing amino acid substitutions were observed in *Pparg* (23), thereby excluding functional differences in peroxisome proliferator-activated receptor  $\gamma$  (PPAR $\gamma$ ) activity. However, four polymorphisms in *Slc21a1* from strain CAST caused amino acid substitutions in SLC21A1 relative to D2; two were conserved residues (T475S, C538S), and thus may affect protein function (see supplementary data). Several polymorphisms were detected in the upstream, putative promoter regions of both candidate genes (supplementary data), but functional analyses of these polymorphisms were beyond the scope of this study. Because both regulatory and coding sequence variations can determine QTL, these data are consistent with the candidacy of *Pparg* and *Slc21a1* for gallstone susceptibility.

## DISCUSSION

Our biliary lipid analyses indicated that the physical-chemical explanation for cholesterol gallstone susceptibil-

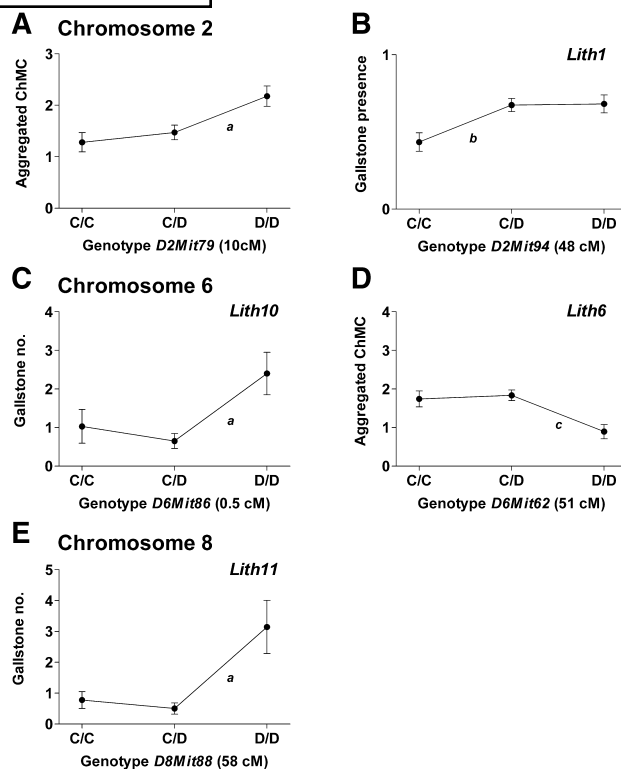
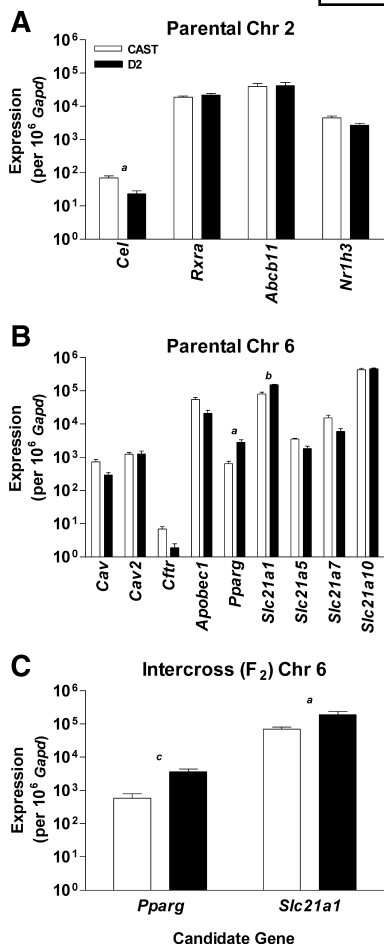


Fig. 5. Allelic contribution to the QTL detected on chrs 2, 6, and 8 for the various gallstone phenotypes. Homozygous CAST alleles are represented by C/C, homozygous D2 alleles by D/D, and heterozygous alleles by C/D. A recessive D2 susceptibility allele determined the QTL for aggregated ChMCs on proximal chr 2 (A). A dominant D2 susceptibility allele determined the QTL for gallstone presence on distal chr 2 (B), which colocalized with the previously identified QTL, *Lith1* (11, 16). A recessive D2 susceptibility allele determined *Lith10*, the new QTL for gallstone number on proximal chr 6 (C). *Lith10* was identified also using the gallstone presence phenotype but was excluded from the plot for clarity. A dominant CAST susceptibility allele determined *Lith6*, the new QTL for the aggregated ChMC phenotype on distal chr 6 (D). A recessive D2 susceptibility determined *Lith11*, the new QTL for gallstone number on chr 8 (E). This QTL was detected with the F<sub>2</sub> lineage as an interacting covariate, so only F<sub>2</sub> mice derived from (D2 × CAST) F<sub>1</sub> mating pairs displayed this QTL. Data represent mean ± SEM (n = 57–146). <sup>a</sup> P < 0.05, C/D versus D/D; <sup>b</sup> P < 0.05, C/C versus C/D; <sup>c</sup> P < 0.01, C/D versus D/D.

ity of male CAST mice was cholesterol hypersecretion. Using an intercross between strains CAST and D2, we detected three new, significant QTL (*Lith6*, *Lith10*, and *Lith11*) and one suggestive QTL (proximal chr 2) for cholesterol gallstone susceptibility. In addition, a significant, fifth QTL coincided with *Lith1*, a QTL identified previously (11, 16). We used three different phenotypes to evaluate gallstone susceptibility (aggregated ChMCs, gallstone number, and gallstone presence). Not surprisingly, these alternative methods of trait evaluation resulted in identification of the same QTL. Unexpectedly, the susceptible strain CAST contributed one susceptibility allele, *Lith6*, whereas the resistant strain D2 contributed the susceptibility alleles at the four remaining QTL. These observations account for the increased gallstone prevalence in F<sub>1</sub>



**Fig. 6.** Hepatic mRNA expression analyses of positional candidate genes identified for the QTL on chrs 2 and 6. mRNA expression was tested in the parental strains (CAST, open; D2, filled) for candidate genes on chr 2 (A) and chr 6 (B). Because F<sub>2</sub> animals inherit unique combinations of parental alleles, mice were selected that were homozygous CAST (open) or homozygous D2 (filled) over the *Lith6* region. The *Lith6* candidates (B) that displayed significant differential expression between strains were tested in the selected F<sub>2</sub> population (C). Parental animals were fed the lithogenic diet for 4 weeks prior to collection of liver tissue, whereas F<sub>2</sub> animals were fed for 10 weeks. Samples were prepared as described in Materials and Methods. Gene-specific oligonucleotide primers were employed to analyze candidate genes using kinetic PCR. Data are reported as the number of target molecules per 10<sup>6</sup> *Gapdh* molecules (mean ± SEM, n = 5 animals per parental strain, mean of three determinations; n = 15 per F<sub>2</sub> genotype, mean of two determinations). The parental strains or genotype groups were compared using Student's *t*-test with Bonferroni posttest for multiple comparisons. <sup>a</sup> *P* < 0.05, <sup>b</sup> *P* < 0.01, <sup>c</sup> *P* < 0.005; [*Nr1h3*, *Apobec1*, and *Pparg* expression data were derived from (23)].

progeny compared with the susceptible parental strain CAST (100% vs. 40% prevalence; Fig. 1).


Seven studies conducted previously in our laboratories indicated suggestive genetic linkage between cholesterol gallstone formation and distal chr 6 using a variety of different strains, which yielded eight QTL [(16–18) and M. C. Carey and B. Paigen, unpublished observations]. Four QTL clustered between 54 cM and 56 cM, whereas the remaining four QTL clustered between 65 and 71 cM (see supplement-

ary data). *Pparg* and *Slc21a1* are located on chr 6 at 52.7 cM and 67.0 cM, respectively. Furthermore, the 95% CIs are generally broad, often an indicator of multiple QTL, in our experience. In this study, both QTL fine-mapping (Fig. 4E) and modeling (Table 2) suggested that two QTL were present on distal chr 6. In addition to *Pparg* and *Slc21a1*, potential candidate genes for this locus included *Apobec1* and a further three Na<sup>+</sup>-independent bile acid and bile salt transporters (32, 33). We confirmed that *Slc21a1* mapped to chr 6 using radiation hybrid mapping, a position consistent with the ENSEMBL mouse genome assembly, the Mouse Genome Database (<http://www.informatics.jax.org/>), and the position of human *SLC21A3* on chr 12p12 (34), which is orthologous to mouse distal chr 6. We can only conclude that the original report that mapped *Slc21a1* to mouse chr X was an artifact. Overall, we determined that *Apobec1*, *Slc21a5*, *Slc21a7*, and *Slc21a10* did not underlie *Lith6*. However, all data were consistent with *Pparg* and *Slc21a1* being candidate genes for *Lith6*. The major finding from the present data is the identification of the new cholesterol gallstone susceptibility QTL, *Lith6*, which is likely to result from two QTL in close proximity.

We postulate that *Pparg* and *Slc21a1* might affect intracellular bile salt concentrations and the availability of cholesterol for biliary secretion. It is now recognized that PPAR $\gamma$  is expressed at low levels in the liver, particularly in cases of obesity, type 2 diabetes, and steatosis (35, 36). One putative role of PPAR $\gamma$  in cholesterol gallstone formation is its derepression of CYP7A1 activity (37). Additionally, troglitazone, a synthetic PPAR $\gamma$  agonist, increased *Cyp7a1* expression when fed to mice (38), although we did not observe differences in *Cyp7a1* mRNA (data not shown). However, because PPAR $\gamma$  is a transcription factor, it probably regulates many more genes than *Cyp7a1* alone. Hepatic basolateral bile salt uptake is predominantly mediated via the Na<sup>+</sup>-dependent taurocholate cotransporting polypeptide, encoded by *Slc10a1* (*Ntcp*), and the Na<sup>+</sup>-independent solute (organic anion) carriers of the *Slc21a* family (32, 33). We observed nucleotide changes in *Slc21a1* that caused four changes in the amino acid sequence of SLC21A1 from CAST compared with D2 (T475S, C538S, V660F, V8I; supplementary data). The alignment of sequences from mouse, rat, and human indicated that within this subfamily, valine and isoleucine are interchangeable at residue 8 and phenylalanine is present in one human member at residue 660, suggesting that such amino acid substitutions may not be important for function. However, threonine and cysteine are conserved at residues 475 and 538, respectively (33), suggesting that these changes might cause a functional variation in protein activity. We speculate that increased CAST SLC21A1 activity (rather than decreased as implied by the CAST mRNA expression data) might increase the availability of bile salts, resulting in a concomitant decrease in cholesterol catabolism [via NRIH4/farnesoid X receptor (FXR)-mediated inhibition], thereby increasing the availability of cholesterol for biliary secretion.

A comment is required regarding our conclusion that

*Nr1h3* was unlikely to determine the QTL that coincided with *Lith1* and the possibility of confounding effects caused by cholic acid (in the lithogenic diet) and NR1H4 (FXR) activation. Previously, it was demonstrated that NR1H4-mediated repression of *Cyp7a1* transcription was able to overcome NR1H3 (LXR $\alpha$ )-mediated activation of *Cyp7a1* transcription (39). However, these data do not support the candidacy of *Nr1h3* for the following reasons: 1) because no QTL was detected in any of the regions harboring *Nr1h4*, *Nr0b2* (*Shp*), or *Nr5a2* (*Lrh*), we inferred that the effect of NR1H4 activation was similar in all F<sub>2</sub> mice; 2) for the locus coincident with *Lith1* to be detected by QTL analysis, it must have affected gallstone susceptibility; and 3) no sequence differences causing amino acid changes were observed in *Nr1h3* (23). Therefore, because NR1H4 activation overcomes NR1H3 activation, and NR1H3 did not display altered function due to inherent amino acid changes, gallstone susceptibility was not affected by NR1H3.

In summary, this study demonstrated that gallstone susceptibility of strain CAST was primarily due to cholesterol hypersecretion, and identified new *Lith* loci on proximal chr 6 (*Lith10*), distal chr 6, (*Lith6*) and distal chr 8 (*Lith11*). *Lith6* is likely a complex locus comprising two linked QTL. However, none of the candidate genes we tested fully accounted for the cholesterol hypersecretion of strain CAST. Elucidation of the underlying mechanisms awaits completion of the construction of overlapping congenic strains, which will enable us to resolve the multiple QTL, to narrow the individual QTL regions, and importantly, to test the hypotheses that were generated in this study. This work further demonstrates the complexity of the genetic origins of cholesterol gallstone formation and its pathobiology and likely will illuminate new approaches toward understanding this very common human disease. 

This work was supported in part by National Institutes of Health Grants DK-51568 (to B.P.), CA-34196 (core grant to The Jackson Laboratory), DK-36588 and DK-52911 (to M.C.C.), and DK-34854 (core grant to Brigham and Women's Hospital). M.A.L. was supported by the American Physiological Society and the American Liver Foundation. H.W. was supported by the Deutsche Forschungsgemeinschaft (grant WI 1905/1-1). The authors are greatly indebted to Dr. Jason Stockwell, Ms. Jennifer Smith, and Ms. Susan Sheehan (The Jackson Laboratory) for consultation on general statistical methods, assistance with graphics, and sequencing of PCR products, respectively. The authors thank David Schultz, Harry Whitmore, and Eric Taylor (The Jackson Laboratory) for colony management.

## REFERENCES

- Small, D. M., M. Bourguès, and D. G. Dervichian. 1966. Ternary and quaternary aqueous systems containing bile salt, lecithin, and cholesterol. *Nature*. **211**: 816–818.
- Dam, H., and F. Hegardt. 1971. The relation between formation of gallstones rich in cholesterol and the solubility of cholesterol in aqueous solutions of bile salts and lecithin. *Z. Ernahrungswiss.* **10**: 239–252.
- Wang, D. Q-H., and M. C. Carey. 1996. Complete mapping of crys-

- tallization pathways during cholesterol precipitation from model bile: influence of physical-chemical variables of pathophysiological relevance and identification of a stable liquid crystalline state in cold, dilute and hydrophilic bile salt-containing systems. *J. Lipid Res.* **37**: 606–630.
- Holzbach, R., C. Corbusher, M. Marsh, and H. Naito. 1976. The process of cholesterol cholelithiasis induced by diet in the prairie dog: a physicochemical characterization. *J. Lab. Clin. Med.* **87**: 987–998.
- Wang, D. Q-H., B. Paigen, and M. C. Carey. 1997. Phenotypic characterization of *Lith* genes that determine susceptibility to cholesterol cholelithiasis in inbred mice: physical-chemistry of gallbladder bile. *J. Lipid Res.* **38**: 1395–1411.
- Wang, D. Q-H., F. Lammert, B. Paigen, and M. C. Carey. 1999. Phenotypic characterization of *Lith* genes that determine susceptibility to cholesterol cholelithiasis in inbred mice. Pathophysiology of biliary lipid secretion. *J. Lipid Res.* **40**: 2066–2079.
- Admirand, W. H., and D. M. Small. 1968. The physicochemical basis of cholesterol gallstone formation in man. *J. Clin. Invest.* **47**: 1043–1052.
- Carey, M. C., and D. M. Small. 1978. The physical chemistry of cholesterol solubility in bile. Relationship to gallstone formation and dissolution in man. *J. Clin. Invest.* **61**: 998–1026.
- Wang, D. Q-H., and M. C. Carey. 1996. Characterization of crystallization pathways during cholesterol precipitation from human gallbladder bile: identical pathways for corresponding model biles with three predominating sequences. *J. Lipid Res.* **37**: 2539–2549.
- Everhart, J. E., F. Yeh, E. T. Lee, M. C. Hill, R. Fabsitz, B. V. Howard, and T. K. Welty. 2002. Prevalence of gallbladder disease in American Indian populations: findings from the Strong Heart Study. *Hepatology*. **35**: 1507–1512.
- Khanuja, B., Y. C. Cheah, M. Hunt, P. M. Nishina, D. Q-H. Wang, H. W. Chen, J. T. Billheimer, M. C. Carey, and B. Paigen. 1995. *Lith1*, a major gene affecting cholesterol gallstone formation among inbred strains of mice. *Proc. Natl. Acad. Sci. USA*. **92**: 7729–7733.
- Paigen, B., and M. C. Carey. 2002. Gallstones. In *The Genetic Basis of Common Diseases*. R. A. King, J. I. Rotter, and A. G. Motulsky, editors. Oxford University Press, New York. 298–335.
- Lammert, F., M. C. Carey, and B. Paigen. 2001. Chromosomal organization of candidate genes involved in cholesterol gallstone formation: a murine gallstone map. *Gastroenterology*. **120**: 221–238.
- Sandler, R. S., J. E. Everhart, M. Donowitz, E. Adams, K. Cronin, C. Goodman, E. Gemmen, S. Shah, A. Avdic, and R. Rubin. 2002. The burden of selected digestive diseases in the United States. *Gastroenterology*. **122**: 1500–1511.
- Wittenburg, H., M. A. Lyons, B. Paigen, and M. C. Carey. 2003. Mapping cholesterol gallstone susceptibility (*Lith*) genes in inbred mice. *Dig. Liver Dis.* **35**: 52–57.
- Paigen, B., N. J. Schork, K. L. Svenson, Y. C. Cheah, J. L. Mu, F. Lammert, D. Q. Wang, G. Bouchard, and M. C. Carey. 2000. Quantitative trait loci mapping for cholesterol gallstones in AKR/J and C57L/J strains of mice. *Physiol. Genomics*. **4**: 59–65.
- Lammert, F., D. Q. Wang, H. Wittenburg, G. Bouchard, S. Hillebrandt, B. Taenzler, M. C. Carey, and B. Paigen. 2002. *Lith* genes control mucin accumulation, cholesterol crystallization, and gallstone formation in A/J and AKR/J inbred mice. *Hepatology*. **36**: 1145–1154.
- Wittenburg, H., F. Lammert, D. Q. Wang, G. A. Churchill, R. Li, G. Bouchard, M. C. Carey, and B. Paigen. 2002. Interacting QTLs for cholesterol gallstones and gallbladder mucin in AKR and SWR strains of mice. *Physiol. Genomics*. **8**: 67–77.
- Lyons, M. A., H. Wittenburg, R. Korstanje, K. Walsh, M. C. Carey, and B. Paigen. 2002. Evaluation of the cholesterol gallstone susceptibility locus *Lith6* in CAST/Ei and DBA/2J inbred strains of mice: evidence for a role of *Pparg* in murine cholelithiasis (Abstract). *Hepatology*. **36**: 458.
- Wittenburg, H., M. A. Lyons, B. Paigen, and M. C. Carey. 2002. FXR, the nuclear bile salt receptor, and ABCG5/8, the putative canalicular cholesterol transporter, as primary genetic determinants of cholesterol gallstone susceptibility: evidence from an intercross of PERA/Ei and I/LnJ strains of mice (Abstract). *Hepatology*. **36**: 342.
- Flint, J., and R. Mott. 2001. Finding the molecular basis of quantitative traits: successes and pitfalls. *Nat. Rev. Genet.* **2**: 437–445.
- Bouchard, G., D. Johnson, T. Carver, M. C. Carey, and B. Paigen. 2001. Multiple new murine models of cholesterol gallstones



- (ChGS): The Jackson Laboratory-Brigham and Women's Hospital strain survey (Abstract). *Gastroenterology*. **120**: 72.
23. Lyons, M. A., H. Wittenburg, R. Li, K. Walsh, G. A. Churchill, M. C. Carey, and B. Paigen. 2003. Quantitative trait loci that determine lipoprotein cholesterol levels in DBA/2J and CAST/Ei inbred mice. *J. Lipid Res.* **44**: 953–967.
  24. Wittenburg, H., M. A. Lyons, R. Li, G. A. Churchill, M. C. Carey, and B. Paigen. 2003. Evidence for FXR and ABCG5/ABCG8 as determinants of cholesterol gallstone susceptibility from a cross of PERA and I Mice. *Gastroenterology*. In press.
  25. Wittenburg, H., F. Lammert, D. Q. Wang, G. A. Churchill, R. Li, G. Bouchard, M. C. Carey, and B. Paigen. 2002. Interacting QTLs for cholesterol gallstones and gallbladder mucin in AKR and SWR strains of mice. *Physiol. Genomics*. **8**: 67–77.
  26. Sen, S., and G. A. Churchill. 2001. A statistical framework for quantitative trait mapping. *Genetics*. **159**: 371–387.
  27. Hagenbuch, B., I. D. Adler, and T. E. Schmid. 2000. Molecular cloning and functional characterization of the mouse organic-anion-transporting polypeptide 1 (Oatp1) and mapping of the gene to chromosome X. *Biochem. J.* **345**: 115–120.
  28. Nathanson, M. H., and J. L. Boyer. 1991. Mechanisms and regulation of bile secretion. *Hepatology*. **14**: 551–566.
  29. Churchill, G. A., and R. W. Doerge. 1994. Empirical threshold values for quantitative trait mapping. *Genetics*. **138**: 963–971.
  30. Schirin-Sokhan, R., S. Matern, and F. Lammert. 2002. Polymorphisms in the human multiligand receptor LRP2 are associated with cholecystolithiasis (Abstract). *Z. Gastroenterol.* **40**: 557.
  31. Christensen, E. I., and H. Birn. 2002. Megalin and cubilin: multifunctional endocytic receptors. *Nat. Rev. Mol. Cell Biol.* **3**: 256–266.
  32. Meier, P. J., and B. Stieger. 2002. Bile salt transporters. *Annu. Rev. Physiol.* **64**: 635–661.
  33. Hagenbuch, B., and P. J. Meier. 2003. The superfamily of organic anion transporting polypeptides. *Biochim. Biophys. Acta.* **1609**: 1–18.
  34. Kullak-Ublick, G. A., U. Beuers, P. J. Meier, H. Domdey, and G. Paumgartner. 1996. Assignment of the human organic anion transporting polypeptide (OATP) gene to chromosome 12p12 by fluorescence in situ hybridization. *J. Hepatol.* **25**: 985–987.
  35. Boelsterli, U. A., and M. Bedoucha. 2002. Toxicological consequences of altered peroxisome proliferator-activated receptor  $\gamma$  (PPAR $\gamma$ ) expression in the liver: insights from models of obesity and type 2 diabetes. *Biochem. Pharmacol.* **63**: 1–10.
  36. Chao, L., B. Marcus-Samuels, M. M. Mason, J. Moitra, C. Vinson, E. Arioglu, O. Gavrilova, and M. L. Reitman. 2000. Adipose tissue is required for the antidiabetic, but not for the hypolipidemic, effect of thiazolidinediones. *J. Clin. Invest.* **106**: 1221–1228.
  37. Miyake, J. H., S. L. Wang, and R. A. Davis. 2000. Bile acid induction of cytokine expression by macrophages correlates with repression of hepatic cholesterol 7 $\alpha$ -hydroxylase. *J. Biol. Chem.* **275**: 21805–21808.
  38. Repa, J. J., S. D. Turley, J. A. Lobaccaro, J. Medina, L. Li, K. Lustig, B. Shan, R. A. Heyman, J. M. Dietschy, and D. J. Mangelsdorf. 2000. Regulation of absorption and ABC1-mediated efflux of cholesterol by RXR heterodimers. *Science*. **289**: 1524–1529.
  39. Xu, G., G. Salen, L. Pan, H. Li, B. M. Forman, M. Ananthanarayanan, S. K. Erickson, B. L. Shneider, S. Shefer, and C. Kuckel. 2003. Manipulating the bile acid pool regulates CYP7A1 by changing FXR activation. In Falk Symposium 129. Bile Acids: From Genomics to Disease and Therapy. G. Paumgartner, D. Keppler, U. Leuschner, and A. Stiehl, editors. Kluwer Academic Publishers, Dordrecht, The Netherlands. 55–60.
  40. Carey, M. C. 1978. Critical tables for calculating the cholesterol saturation of native bile. *J. Lipid Res.* **19**: 945–955.